Fig. 1. Schematic Protocol of Antibody Proteomics

Table 1. Protein Expression of Identified Drug Target Candidates Using Tissue Microarray

Target candidate	Positive ratio	
	Healthy mammal	Breast cancer
Her2 (Control)	0/15 (0%)	53/189 (28%)
IkappaBR	3/15 (20%)	22/189 (12%)
SPATA5 protein	0/15 (0%)	0/189 (0%)
beta actin variant	0/15 (0%)	0/189 (0%)
TRAIL-R2	0/15 (0%)	119/189 (63%)
RREB-1	1/15 (6%)	83/189 (44%)
FLJ31438 protein	0/15 (0%)	0/189 (0%)
hPAK65	0/15 (0%)	0/189 (0%)
Cytokeratin 8	0/15 (0%)	137/189 (73%)
XRN1 protein	0/15 (0%)	0/189 (0%)
Jerky protein homolog-like	0/15 (0%)	0/189 (0%)
EPH receptor A10 (EphA10)	0/15 (0%)	93/189 (49%)

EphA10 positive ratio in Her-2 Negative breast cancer patient
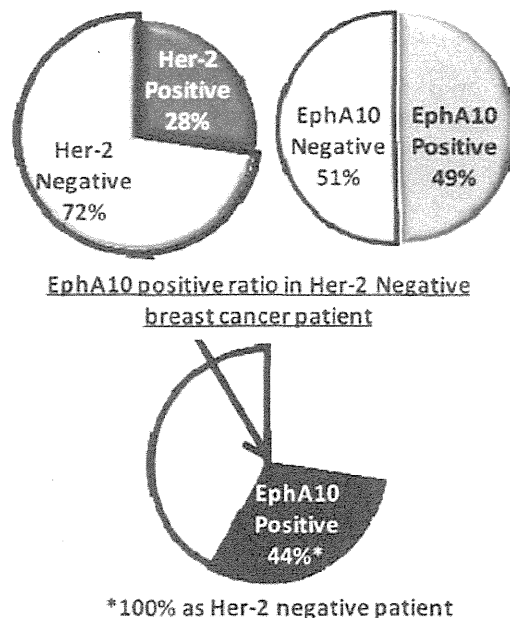
*100% as Her-2 negative patient

Fig. 2. EphA10 Expression in Breast Cancer Patients

の約半数に発現する創薬ターゲットとしても有用性の高い分子であることが明らかになった (Fig. 2).

3. 血管プロテオミクス

このように創薬ターゲットとしての分子探索にプロテオミクスの手法を用いることは極めて有用であり，今後数多くの標的分子を発見できる可能性を示唆している．その一方で，現在の抗体医薬の標的分子のほとんどが，膜タンパク質及び分泌タンパク質を標的とした分子標的治療薬である事実からも，抗体医薬を用いる限り，現在の技術背景では，細胞質

内に存在するタンパク質を標的にするのは数多くの問題点があると考えられている．[10] したがって，抗体医薬の開発を念頭に置く場合には，膜タンパク質や分泌タンパク質を標的にすることが実用化において最も近道であると考えられる．そこで，細胞膜タンパク質，及び細胞外マトリクス等の分泌タンパク質の発現挙動の解析のために，全身の血管をビオチン化試薬にてラベル化し，疾患組織にある血管内皮

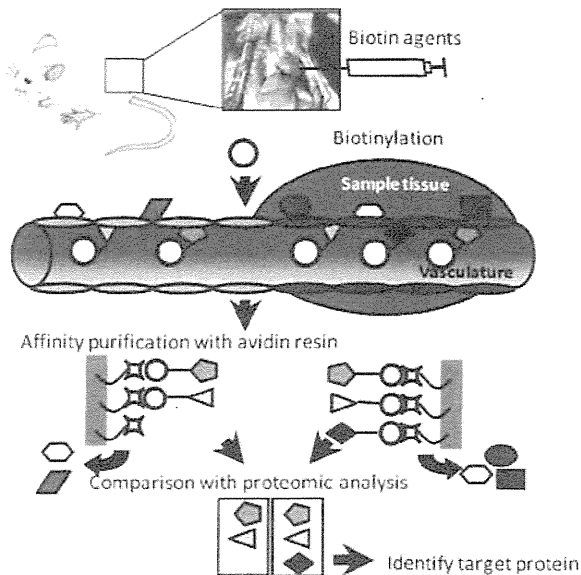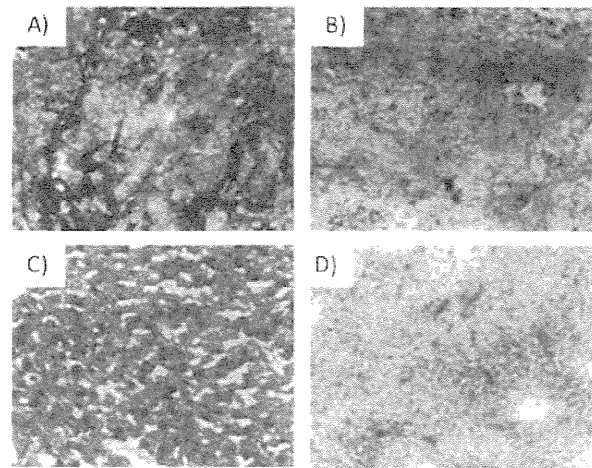Fig. 3.　Schematic Protocol of Vasculature Proteomics

Fig. 4.　BST-2 Expression in Metastatic Lymphoma
　　(A) Liver metastatic tumor; (B) Spleen metastatic tumor; (C) Normal liver; (D) Normal spleen. Immunohistochemistry were performed by using anti-BST-2 polyclonal antibody. Tumor vascular regions were stained (dark gray) but not normal tissues.

細胞の膜タンパク質並びに分泌タンパク質を効率よく回収・精製可能な *in vivo* biotinylation 法を活用し血管プロテオームを行うことにした.[11] Figure 3 にその概要を示す. この *in vivo* biotinylation 法は, 細胞膜タンパク質を解析する場合に, 現在汎用されている組織抽出後の膜タンパク質を回収する方法とは異なり, 直接組織細胞の外側からラベル化を行うため, 小胞膜のコンタミネーションのリスクを回避できる. 当然のことながら, 細胞外の膜タンパク質等を選択的にビオチンラベルするため, 解析結果から得られたタンパク質候補に対するモノクローナル抗体は, 通常の方法でプロテオーム解析して得られたタンパク質候補 (多くの場合, シャペロンタンパク質やヒートショックタンパク質といった細胞内タンパク質) に対する抗体よりも, 基礎医学・臨床医学的な有用性に優れていることは言うまでもない. そのうえ, 血管側からビオチン化しているため, 組織中の血管内皮細胞がより効率よくラベル化されており, 抗体医薬の開発には極めて有用な方法であると考えられる.

この血管プロテオミクスを担がんマウスモデルに対して行い, 転移性リンパ腫の治療に向けた抗原の探索を行った.[12] 具体的には, 抗体のラベル化等に用いるビオチン化試薬を, *in vivo* に直接投与・環流することで, 組織に存在する血管を直接ラベル化した. その結果, 腫瘍血管での発現がこれまでにも報告されている Transferrin 受容体が同定された一方, これまで知られていなかった新しいがん血管関連抗原として BST-2 の発現を見い出した (Fig. 4).[12] BST-2 は, 肝臓や脾臓に転移したリンパ腫の血管部位に特異的に発現しており, これを標的としたがん治療薬の開発が期待される. 実際に, この BST-2 に対する抗体を投与することで, 腫瘍の増殖が抑制される結果も見い出しており, 今後これらを利用した抗体医薬の開発も期待されるところである.

4.　結論と展望

抗体プロテオミクス技術はプロテオミクスと抗体工学の技術を組み合わせ, さらに組織マイクロアレイによるバリデーションを迅速に行うことで, 標的分子を迅速にバリデーションできる技術である. この技術により, これまで標的分子の探索から発現解析までの膨大な時間と労力を, わずか 2–3 週間程度の期間で達成できる極めて有用な技術として開発することができた. また先述したように血管プロテオミクスは, 個体レベルでのプロテオミクスを可能とするうえ, 細胞膜タンパク質及び細胞外マトリクス等の分泌タンパク質を効果的にラベル化できる方法であり, 細胞質内タンパク質のコンタミネーションを回避できるという圧倒的な利点を有している. この 2 つのプロテオミクス技術を融合することで, 疾患における創薬ターゲットの同定に留まらず, 新しい抗体医薬の開発法として利用することを考えてい

る．今後，本方法を用いて同定された抗原に対する抗体を作製することで，バイオマーカーの検出や評価に利用できるものと期待されるとともに，タンパク質の発現挙動解析，並びに同定作業を現在も進めているところであり，プロテオミクスによる解析基盤の確立に向けた開発・最適化を今後も行う予定である．

REFERENCES

1) Kramer R., Cohen D., *Nat. Rev. Drug Discov.*, **3**, 965–972 (2004).

2) Butte A., *Nat. Rev. Drug Discov.*, **1**, 951–960 (2002).

3) Latterich M., Schnitzer J. E., *Nat. Biotechnol.*, **29**, 600–602 (2011).

4) Rifai N., Gillette M. A., Carr S. A., *Nat. Biotechnol.*, **24**, 971–983 (2006).

5) Goodman M., *Nat. Rev. Drug Discov.*, **8**, 837 (2009).

6) Nelson A. L., Reichert J. M., *Nat. Biotechnol.*, **27**, 331–337 (2009).

7) Yamashita T., Utoguchi N., Suzuki R., Nagano K., Tsunoda S., Tsutsumi Y., Maruyama K., *Yakugaku Zasshi*, **130**, 479–485 (2010).

8) Giltnane J. M., Rimm D. L., *Nat. Clin. Pract. Oncol.*, **1**, 104–111 (2004).

9) Imai S., Nagano K., Yoshida Y., Okamura T., Yamashita T., Abe Y., Yoshikawa T., Yoshioka Y., Kamada H., Mukai Y., Nakagawa S., Tsutsumi Y., Tsunoda S., *Biomaterials*, **32**, 162–169 (2011).

10) Williams B. R., Zhu Z., *Curr. Med. Chem.*, **13**, 1473–1480 (2006).

11) Roesli C., Neri D., *J. Proteomics*, **73**, 2219–2229 (2010).

12) Schliemann C., Roesli C., Kamada H., Borgia B., Fugmann T., Klapper W., Neri D., *Blood*, **115**, 736–744 (2010).

Plasma membrane proteomics identifies bone marrow stromal antigen 2 as a potential therapeutic target in endometrial cancer

Takuhei Yokoyama[1,2], Takayuki Enomoto[1], Satoshi Serada[2], Akiko Morimoto[1,2], Shinya Matsuzaki[1,2], Yutaka Ueda[1], Kiyoshi Yoshino[1], Masami Fujita[1], Satoru Kyo[3], Kota Iwahori[2], Minoru Fujimoto[2], Tadashi Kimura[1] and Tetsuji Naka[2]

[1] Department of Obstetrics and Gynecology, Osaka University Graduate School of Medicine, Osaka, Japan
[2] Laboratory for Immune Signal, National Institute of Biomedical Innovation, Osaka, Japan
[3] Department of Obstetrics and Gynecology, Kanazawa University Graduate School of Medicine, Kanazawa, Japan

This report utilizes a novel proteomic method for discovering potential therapeutic targets in endometrial cancer. We used a biotinylation-based approach for cell-surface protein enrichment combined with isobaric tags for relative and absolute quantitation (iTRAQ) technology using nano liquid chromatography–tandem mass spectrometry analysis to identify specifically overexpressed proteins in endometrial cancer cells compared with normal endometrial cells. We identified a total of 272 proteins, including 11 plasma membrane proteins, whose expression increased more than twofold in at least four of seven endometrial cancer cell lines compared with a normal endometrial cell line. Overexpression of bone marrow stromal antigen 2 (BST2) was detected and the observation was supported by immunohistochemical analysis using clinical samples. The expression of BST2 was more characteristic of 118 endometrial cancer tissues compared with 59 normal endometrial tissues ($p < 0.0001$). The therapeutic effect of an anti-BST2 antibody was studied both in vitro and in vivo. An anti-BST2 monoclonal antibody showed in vitro cytotoxicity in BST2-positive endometrial cancer cells via antibody-dependent cell-mediated cytotoxicity and complement-dependent cytotoxicity. In an in vivo xenograft model, anti-BST2 antibody treatment significantly inhibited tumor growth of BST2-positive endometrial cancer cells in an NK cell-dependent manner. The anti-BST2 antibody had a potent antitumor effect against endometrial cancer both in vitro and in vivo, indicating a strong potential for clinical use of anti-BST2 antibody for endometrial cancer treatment. The combination of biotinylation-based enrichment of cell-surface proteins and iTRAQ analysis should be a useful screening method for future discovery of potential therapeutic targets.

Anticancer monoclonal antibodies are a growing family of novel agents applied in the treatment regimens for hematopoietic and solid tumors. Antibody-based therapeutic agents against CD20 or Her2 have been successfully clinically developed and have significant therapeutic effects.[1,2] Tumor-associated antigens which are easily accessible from the tumor neovasculature are particularly attractive for intravenously-administered antibody-based therapeutic agents. During the last decade, several new technologies for high-throughput screening have identified many potential therapeutic targets. Thus far, no single approach or combination of methods has emerged as the preferred paradigm. It is clear that new tools and strategies are needed so that tumor-associated antigens can be screened efficiently.

Proteomic methods can now be tailored to search directly for targetable cell-surface proteins that distinguish cancer cells from normal cells. The complexity and concentration of individual proteins in the sample are crucial when performing proteomic analyses because abundant proteins, such as cytoskeletal proteins, may hinder the detection of low abundance proteins, such as plasma membrane proteins.[3] One way to enrich the potentially accessible cell-surface proteins is by whole cell protein tagging followed by affinity purification. A method for enrichment of such cell-surface proteins

What's new?

In this study, we have used a biotinylation-based approach for cell-surface protein enrichment combined with iTRAQ technology to identify and quantify membrane proteins which might represent potential therapeutic targets of endometrial cancer. A monoclonal antibody targeting BST2, one of the proteins identified in the iTRAQ analysis, have a potent antitumor effect against endometrial cancer both *in vitro* and *in vivo*, indicating a strong potential for clinical use of anti-BST2 antibody for endometrial cancer treatment.

via their biotinylation and affinity purification has been reported.[4,5] In most cases, concentrated cell-surface proteins are separated by SDS-PAGE and the enzymatically digested peptides are analyzed by mass spectrometry, while highly accurate quantitative data cannot be obtained by using this method. To acquire more quantitative information, stable isotope labeling using amino acids in cell culture (SILAC) based quantitative proteomics has been used, with high quantitative accuracy; however, the SILAC approach has the limitation that only a maximum of three samples can run in any single analysis.[6,7] Compared with SILAC, the more recently developed isobaric tags for relative and absolute quantitation (iTRAQ) technology has a distinct advantage regarding sample number handling capability in a single analysis, because iTRAQ can compare up to eight samples simultaneously.[7,8]

Endometrial cancer is the most common malignant tumor of the female genital tract. Its incidence varies among regions; it is overall the fourth most common malignancy in North America.[9] In general, the prognosis of these patients is excellent as the majority present with early-stage disease that is confined to the uterus at the time of diagnosis, which is followed by simple hysterectomy, leading to a 5-year survival rate of 84%.[9] Unfortunately, those women who present with recurrent or advanced-stage disease have a much poorer prognosis, with a median survival of less than a year.[10] To date, combination chemotherapy of cisplatin, doxorubicin, and paclitaxel has demonstrated the greatest efficacy.[10–12] However, these cytotoxic agents are associated with intolerable side effects and infrequent sustainable remission.[11,12] Thus, new and more effective targeted therapies for endometrial cancer are urgently needed. However, thus far the search for agents effective in the treatment of either recurrent or advanced endometrial cancer has been disappointing.[12]

Aiming for the identification of surface-accessible tumor antigens best suitable for antibody-based therapeutic intervention, it is important to analyze plasma membrane proteins known to be involved in endometrial cancer. For this purpose, we have utilized a novel proteomic technology by combining biotinylation-based approach for cell membrane enrichment and iTRAQ technology using nano liquid chromatography–tandem mass spectrometry (LC-MS/MS) analysis. In this study, one normal endometrial cell line (EM-E6/E7/TERT cells, immortalized normal endometrial cells) and seven endometrial cancer cell lines were used as a comparative model for studying the plasma membrane proteins related to endometrial cancer. Among 272 proteins identified

by iTRAQ analysis, bone marrow stromal antigen 2 (BST2) was investigated in more detail. By immunohistochemical analysis using actual clinical specimens, we found that the expression level of BST2 was significantly higher in endometrial cancer tissues compared with normal endometrial tissues. An anti-BST2 antibody showed potent antibody-dependent cell-mediated cytotoxicity (ADCC) and complement-dependent cytotoxicity (CDC) against BST2-positive endometrial cancer cells *in vitro*. In an *in vivo* xenograft model, anti-BST2 antibody treatment significantly inhibited tumor growth.

Taken together, our strategy of screening cell-surface tumor-specific antigens might be useful for identifying new therapeutic targets.

Material and Methods

Cell lines and cultures

We previously established an immortalized normal endometrial cell line (EM-E6/E7/TERT cells).[13,14] Nine human endometrial cancer cell lines (HEC-1, HEC-1A, HEC-6, HEC-88nu, HEC-108, HEC-116, HEC-251, SNG-II, and SNG-M cells) were obtained from the Japanese Collection of Research Bioresources (JCRB, Osaka, Japan), where they were tested and authenticated on June 30, 2011. The method used for testing was multiplexed PCR amplification of eight short tandem repeat loci (TH01, D5S818, D13S317, D7S820, D16S539, CSF1PO, vWA, and TPOX) and amelogenin was performed using the PowerPlex^{TM}16 System (Promega, Madison, WI). PCR-amplified fragments were analyzed with an ABI PRISM 310 Genetic Analyzer (Applied Biosystems, Foster City, CA). Then the fragments were typed based on allelic ladders. EM-E6/E7/TERT cells were maintained in a 1:1 mixture of DMEM and Ham's F12 medium (Wako Pure Chemical Industries, Osaka, Japan) supplemented with 10% FBS (HyClone Laboratories, Logan, UT) and 1% penicillin-streptomycin (Nacalai Tesque, Kyoto, Japan) at 37°C under a humidified atmosphere of 5% CO_2. HEC-1, HEC-1A, HEC-6, HEC-88nu, HEC-108, HEC-116, and HEC-251 cells were maintained and propagated in DMEM (Wako Pure Chemical Industries) supplemented with 10% FBS and 1% penicillin-streptomycin. SNG-II and SNG-M cells were maintained in Ham's F12 (Invitrogen, Carlsbad, CA) with 10% FBS and 1% penicillin-streptomycin.

Biotinylation of bovine serum albumin (BSA)

BSA (30 μM) was biotinylated with a 100-fold molar excess of sulfosuccinimidyl 2-(biotinamido)-ethyl-1,3-dithiopropionate

(sulfo-NHS-SS-biotin; Pierce, Rockford, IL) and desalted as described previously.[15]

Capture of cell-surface proteins

To isolate cell-surface proteins, the normal endometrial cell line (EM-E6/E7/TERT cells) and seven endometrial cancer cell lines (HEC-1, HEC-1A, HEC-6, HEC-108, HEC-116, HEC-251, and SNG-II cells) were grown to approaching confluency (up to 90%) in three 15 cm dishes. Cells were washed three times with prewarmed PBS and then the cell-surface proteins were biotinylated for 15 min at room temperature with 15 ml of 500 μM sulfo-NHS-SS-biotin solution dissolved in PBS. The residual biotinylation reagent was quenched with 5 mM lysine for 5 min at room temperature. After biotinylation, the cells were washed with PBS twice, harvested by scraping, and collected by centrifugation (1,500 rpm, 4°C, 5 min). Detailed methods of extraction and purification of biotinylated cell-surface proteins are described in the Supporting Information Materials and Methods section.

iTRAQ labeling

Trypsin-digested peptides were dissolved in 5 μl of 9.8 M urea and 20 μl of 1M TEAB. Samples were labeled with the iTRAQ reagent according to the manufacturer's protocol (Applied Biosystems). EM-E6/E7/TERT cells were labeled with iTRAQ reagent 113, HEC-1 cells with 114, HEC-1A cells with 115, HEC-6 cells with 116, HEC-108 cells with 117, HEC-116 cells with 118, HEC-251 cells with 119, and SNG-II cells with 121. The labeled peptide samples were then pooled and desalted with Sep-Pak Light C18 Cartridges (Waters, Manchester, UK) and peptides were dried in a centrifugal concentrator (Micro Vac MV-100, Tomy, Tokyo, Japan) before strong cation exchange (SCX) fractionation.

SCX fractionation

In order to remove excess unreacted iTRAQ reagent and to simplify the complexity of the peptide mixture, the labeled peptide mixtures were purified and fractionated using SCX column (SCX, PolySulfoethyl A column, 2.1 × 150 mm, 5 μm, 300 Å) on an Agilent 1200 HPLC system. Detailed information is provided in the Supporting Information Materials and Methods section.

Mass spectrometric analysis

Nano LC-MS/MS analyses were performed on an LTQ-Orbitrap XL (Thermo Fisher Scientific, Waltham, MA) equipped with a nano-ESI source and coupled to a Paradigm MG4 pump (Michrom Bioresources, Auburn, CA) and autosampler (HTC PAL, CTC Analytics, Zwingen, Switzerland). Detailed information is provided in the Supporting Information Materials and Methods section.

iTRAQ data analysis

Protein identification and quantification for iTRAQ analysis was carried out using Proteome Discoverer software (v. 1.1)

(Thermo Fisher Scientific) against Swiss Prot human protein database (SwissProt_2011_11, 533,049 entries). Taxonomy was set to *Homo sapiens* (20,326 entries) or mammalian (65,656 entries). Search parameters for peptide and MS/MS mass tolerance were 10 ppm and 0.8 Da, respectively, with allowance for two missed cleavages made from the trypsin digest. Carbamidomethylation (Cys) and iTRAQ8plex (Lys, N-terminal) were specified as static modifications, whereas CAMthiopropanoyl (Lys, N-terminal), iTRAQ8plex (Tyr), and oxidation (Met) were specified as variable modifications in the database search. The false discovery rate of 1% was calculated by Proteome Discoverer based on a search against a corresponding randomized database. Relative protein abundances were calculated using the ratio of iTRAQ reporter ion in the MS/MS scan. For subcellular localization, all the proteins identified in this analysis were analyzed using the UniprotKB (available at: http://www.uniprot.org/) and Ingenuity Pathway Analysis software (Ingenuity Systems, Redwood City, CA).

Quantitative reverse transcription-PCR (qRT-PCR) analysis

To confirm the altered expression of BST2 in endometrial cancer, the normal endometrial cell line (EM-E6/E7/TERT cells) and nine endometrial cancer cell lines (HEC-1, HEC-1A, HEC-6, HEC-88nu, HEC-108, HEC-116, HEC-251, SNG-II, and SNG-M cells) were subjected to qRT-PCR. Total RNA was extracted using an RNeasy Mini Kit (Qiagen, Valencia, CA) and cDNAs were synthesized with a QuantiTect Reverse Transcription Kit (Qiagen), all according to the manufacturers' instructions. qRT-PCR was performed using SYBR Premix Ex taq (Takara Bio, Shiga, Japan) and an ABI 7900HT real-time PCR instrument (Applied Biosystems). β-Actin was used as a housekeeping gene for normalization of quantitative real-time PCR analysis. The primer sequences and the expected sizes of PCR products were as follows: BST2, forward primer 5′-GGAGGAGCTTGAGGGAGAG-3′ and reverse primer 5′-CTCAGTCGCTCCACCTCTG-3′, 75 bp; β-actin, forward primer 5′-AGCCTCGCCTTTGCCGA-3′ and reverse primer 5′-CTGGTGCCTGGGGCG-3′, 174 bp. Relative quantitation of gene expression was performed using the standard curve method as outlined by Applied Biosystems. Experimental conditions were tested in triplicate and three independent experiments were performed.

Fluorescence activated cell sorting (FACS) analysis

Cells were washed twice in PBS (Nacalai Tesque) and detached with 0.02% EDTA solution (Nacalai Tesque). Cells were washed twice with cold FACS buffer (PBS supplemented with 1% FBS and 0.1% sodium azide) and then incubated with mouse anti-human BST2 antibody (Biolegend, San Diego, CA) at a 1:100 dilution and labeled with Alexa Fluor 488-labeled donkey anti-mouse IgG antibody (Invitrogen). Stained cells were analyzed using a FACS Canto cytometer (Becton Dickinson, Mountain View, CA) and the results were analyzed using FlowJo software (Tree Star, Stanford, CA).

Patients and tissue samples

The formalin-fixed, paraffin-embedded tissue sections of 59 cases of normal endometrium and 118 cases of endometrial cancer were obtained from 177 patients who underwent surgical resections at Osaka University Hospital, Japan, between 1998 and 2007. Cases of normal endometrium were obtained from 59 patients who underwent simple hysterectomy for benign indications such as leiomyoma and uterine prolapse. Histological features of the tissues were reviewed by board-certified pathologists. The degree of histological differentiation and surgical pathological staging of 118 cases of endometrial cancer were assigned according to the 1988 recommendations of International Federation of Gynecology and Obstetrics. A summary of clinicopathological information for these patients is shown in Supporting Information Table S1. Written informed consent was obtained for all the cases and the experimental protocol was approved by the ethics committees of Osaka University and National Institute of Biomedical Innovation.

Immunohistochemistry

Sections were prepared from formalin-fixed, paraffin-embedded tissue specimens, deparaffinized, and rehydrated in graded alcohols. Immunohistochemical staining for BST2 was performed using the avidin-biotin-peroxidase complex (ABC) method using a rabbit polyclonal anti-BST2 antibody (Sigma-Aldrich, St. Louis, MO) and the Vectastain ABC kit (Vector Laboratories, Burlingame, CA) according to the manufacturer's protocol. Immunostained sections were photographed with an Olympus FSX100 (Olympus, Tokyo, Japan). Detailed information is provided in the Supporting Information Materials and Methods section.

Evaluation of immunohistostaining

Immunostainings were scored according to the intensity of the staining (no staining = 0, weak staining = 1, moderate staining = 2, strong staining = 3) and the extent of stained cells (0–9% = 0, 10–40% = 1, 41–70% = 2, 71–100% = 3). The final immunohistochemistry (IHC) score was determined by multiplying the intensity score (0, 1, 2, or 3) with the positivity score (0, 1, 2, or 3), resulting in a maximum score of 9. Three independent gynecologic oncologists (Y.U., K.Y., and M.F.), blinded to the histological data, analyzed the stained sections using an Olympus BH2 microscope (Olympus). In case of disagreement, the staining results were re-evaluated by careful discussion until a consensus was reached.

Cell proliferation assay

Endometrial cancer cells plated in 96-well plates (1,000 cells per well) were grown in their respective media for 24, 48, or 72 hr after the addition of antibody or small interfering RNA (siRNA) transfection. At each time point, cell proliferation was assessed by a WST-8 assay according to the manufacturer's protocol (Nacalai Tesque). Detailed information for these assays can be found in the Supporting Information Materials and Methods section.

ADCC assay

ADCC was measured by calcein-acetoxymethyl ester (calcein-AM) release assay, with sensitivity similar to the traditional ^{51}Cr release assay.[16,17] Detailed information for this assay can be found in the Supporting Information Materials and Methods section.

CDC assay

CDC was evaluated using a ^{51}Cr release assay.[18] Detailed information for this assay can be found in the Supporting Information and Methods section.

Tumor xenograft and antibody therapy

Healthy female severe combined immunodeficient (SCID) and nonobese diabetic (NOD)/SCID mice at 8 weeks of age were obtained from Charles River Japan (Yokohama, Japan) and maintained in a specific pathogen-free facility. For subcutaneous xenograft experiments, SCID mice were inoculated subcutaneously with 5×10^6 HEC-88nu or SNG-II cells in a total volume of 50 µl of 1/1 (v/v) PBS/Matrigel (Becton Dickinson) into the abdomen. NOD/SCID mice were inoculated with 5×10^6 HEC-88nu cells. PBS, isotype control (mouse IgG2aκ, Sigma-Aldrich), or mouse anti-human BST2 antibody (clone 1B4: Chugai Pharmaceutical) was administered intraperitoneally at a dose of 5 mg/kg (SNG-II) or 10 mg/kg (HEC-88nu) in 400 µl of PBS. Six mice were used per group. The first dose was given on day 4 (SNG-II) or 9 (HEC-88nu) and continued twice weekly for 4 weeks. Tumors were measured twice weekly from days 4 (SNG-II) or 9 (HEC-88nu) using vernier calipers throughout the study. Tumor volumes were calculated using the following formula: tumor volume (mm^3) = length × width × height. After 8 (HEC-88nu) or 12 (SNG-II) weeks, tumors were resected and weighted. All animal experiments were conducted according to the institutional ethical guidelines for animal experimentation of the National Institute of Biomedical Innovation.

Statistical analysis

For immunohistochemistry, statistical significance of difference between normal endometrium and endometrial cancer was analyzed by the nonparametric Mann–Whitney U test. Differences in the *in vitro* cytotoxic assay were determined by using the Kruskal–Wallis test followed by the Steel procedure. For all subcutaneous tumor comparisons, groups were analyzed using the Kruskal–Wallis test followed by the Steel-Dwass procedure.

Results

Protein expression profiles in normal endometrium and endometrial cancer

To identify potential therapeutic targets of endometrial cancer, we performed comparative protein expression profiling between normal endometrium (EM-E6/E7/TERT cells) and

endometrial cancer (HEC-1, HEC-1A, HEC-6, HEC-108, HEC-116, HEC-251, and SNG-II cells) at the cell surface level. We identified a total of 272 proteins by a biotinylation-based approach for cell membrane enrichment combined with iTRAQ technology using nano LC-MS/MS analysis. The complete list of all the proteins identified is shown in Supporting Information Table S2. The list of proteins identified with single peptide is provided in Supporting Information Table S3. MS/MS spectra of all single-peptide-based assignments with masses detected as well as fragment assignments are presented in Supporting Information Table S4. The raw MS data of this analysis is publicly available for download from PeptideAtlas (available at: http://www.peptideatlas.org/PASS/PASS00032). To correct the error of quantitation during chromatographic procedures, we added the equivalent moles of the sulfo-NHS-SS-biotin labeled BSA into the each sample as an internal standard. The iTRAQ ratio of BSA (0.873 to 1.131, Supporting Information Table S3) was used for the correction of quantitation information accurately. According to the annotation from UniprotKB and Ingenuity Pathway Analysis, 139 proteins (51% of the identified proteins) were located in the plasma membrane (Fig. 1a). Among these 139 plasma membrane proteins identified, 11 proteins were increased more than twofold in at least four of seven endometrial cancer cell lines compared with the normal endometrial cell line (Table 1). As expected, neural cell adhesion molecule L1, a plasma membrane protein previously known to be overexpressed in endometrial cancer, was identified again. Interestingly, BST2 was found to show one of the most significant differences in expression between normal endometrial cells and endometrial cancer cells, making it a prime target.

Confirmatory studies by qRT-PCR and FACS

To confirm the altered expression of BST2 in endometrial cancer, we first evaluated its transcripts by qRT-PCR in the normal endometrial cell line (EM-E6/E7/TERT cells) and nine endometrial cancer cell lines (HEC-1, HEC-1A, HEC-6, HEC-88nu, HEC-108, HEC-116, HEC-251, SNG-II, and SNG-M cells). BST2 mRNA expression was clearly detected in seven of the nine endometrial cancer cell lines, while the normal endometrial cell line showed no detectable expression of BST2 transcripts (Fig. 1b).

We then evaluated the expression of BST2 at the protein level and confirmed the surface localization of BST2 by FACS analysis. Protein expression of BST2 was very weak in EM-E6/E7/TERT cells. In contrast, a considerably higher level of BST2 protein expression was detected in six of the nine endometrial cancer cell lines on the cell surface (Fig. 1c). Together our data demonstrate that BST2 was overexpressed in endometrial cancer cells at both the mRNA and protein level; this was consistent with our iTRAQ analysis.

Validation study by IHC

As a validation study, immunohistochemical analyses were performed by examination of the BST2 expression pattern

in paraffin-embedded tissue samples (Supporting Information Table S1). Representative immunohistochemical staining of BST2 in tissue sections from patients revealed intense BST2 staining in endometrial cancer compared with normal endometrium (Fig. 2a). In addition, immunohistochemical analyses showed membranous immunoreactivity in endometrial cancer cells, indicating that the localization of BST2 was at cell surface. We observed significantly stronger positive staining of BST2 in tissue sections from patients with endometrial cancer compared with normal endometrium ($p < 0.0001$) (Fig. 2b). In 118 endometrial cancer specimens, moderately to strongly positive staining (IHC score = 3–9) was detected in 71.2% of specimens (84 of 118), whereas only 1.7% (1 of 59) were positive in the normal endometrial specimens. There were no significant differences in BST2 immunohistochemical staining among endometrial cancer tissues according to their degree of histological differentiation or surgical pathological staging ($p = 0.77$ and 0.06, respectively, by the Kruskal–Wallis test). There were no significant differences in BST2 staining among normal proliferative-phase, secretory-phase, and atrophic endometrium ($p = 0.82$ by the Kruskal–Wallis test). These results indicate that BST2 was overexpressed on the cell surface of endometrial cancer tissues much more frequently than in normal endometrium, raising the possibility that BST2 might represent a potential therapeutic target.

BST2-siRNA and anti-BST2 antibody treatment *in vitro*

To examine whether the BST2 expression contributes to cell proliferation of endometrial cancer cells, the effect of BST2-siRNA treatment in four of the endometrial cancer cell lines expressing BST2 (HEC-6, HEC-88nu, HEC-116, and SNG-II cells) was evaluated using the WST-8 assay. To ensure silencing efficiency, BST2 expression was analyzed by FACS analysis after 48 hr of siRNA transfection. The two siRNAs targeting BST2 (Hs_BST2_1 and Hs_BST2_5) had a similar silencing effect on the protein level (Supporting Information Fig. S1). There were no significant differences in cell proliferation among BST2-siRNA and control-siRNA treated cells (Fig. 3a). Similarly, anti-BST2 antibody treatment did not affect *in vitro* cell proliferation (Fig. 3b).

We subsequently examined whether an anti-BST2 antibody can induce ADCC among endometrial cancer cells using the calcein-AM release assay. To study the specificity of anti-BST2 antibody-mediated ADCC against BST2-expressing target cells, an ADCC assay was performed using a BST2-expressing endometrial cancer cell line (HEC-88nu cells) and a BST2-negative cell line (HEC-1 cells). As shown in Figure 3c, HEC-88nu cells treated with the anti-BST2 antibody showed specific lysis *via* ADCC ($p = 0.045$), whereas the anti-BST2 antibody showed no lytic activity against HEC-1 cells.
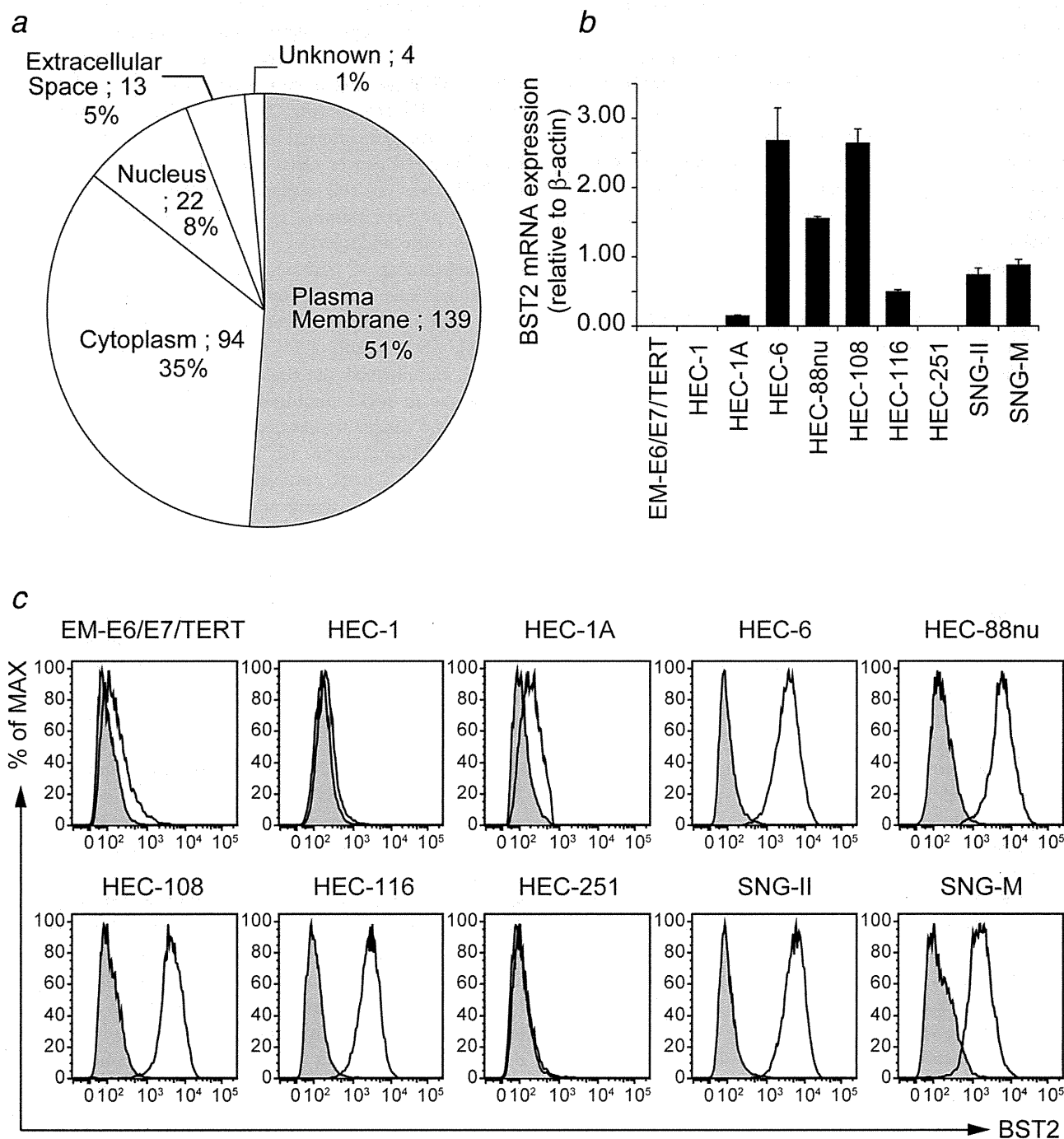
Figure 1. (*a*) Subcellular localization of the identified 272 proteins analyzed by UniprotKB and Ingenuity Pathway Analysis. (*b*) Confirmation of iTRAQ results by qRT-PCR. qRT-PCR was used to quantify BST2 mRNA; β-actin was used as the internal control. Data are mean ± SEM of three independent experiments, each performed in triplicate. BST2 mRNA expression was not detected in the normal endometrial cell line (EM-E6/E7/TERT cells), but seven of nine endometrial cancer cell lines exhibited positive expression of BST2 mRNA. (*c*) Confirmation of iTRAQ results by FACS analysis. The shaded histogram profile indicates the isotype control, and the open histogram indicates the anti-BST2 antibody staining results.

We also examined CDC exhibited by the anti-BST2 antibody. Figure 3*d* shows that the BST2-expressing endometrial cancer cell line (HEC-88nu cells), but not the BST2-negative cell line (HEC-1 cells), was sensitive to CDC ($p = 0.045$).

Therapeutic effect of the anti-BST2 antibody *in vivo*

To evaluate the therapeutic efficacy of anti-BST2 antibody therapy, *in vivo* studies were performed using an endometrial cancer xenograft model. SCID mice injected with either

Table 1. Plasma membrane proteins overexpressed in endometrial cancer cells

Accession number	Protein name	No. peptides used for identification	iTRAQ ratio						
			HEC-1	HEC-1A	HEC-6	HEC-108	HEC-116	HEC-251	SNG-II
O14672	Disintegrin and metalloproteinase domain-containing protein 10	5	1.670	1.271	2.032	3.175	2.824	3.958	1.364
P11279	Lysosome-associated membrane glycoprotein 1	1	0.398	3.017	5.745	8.722	4.307	5.239	1.727
P25942	Tumor necrosis factor receptor superfamily member 5	2	2.518	5.353	7.796	6.438	8.526	2.747	n.d.
P31431	Syndecan-4	5	n.d.	n.d.	0.949	11.644	2.905	4.396	8.121
P32004	Neural cell adhesion molecule L1	26	1.211	0.905	2.171	9.025	2.603	13.756	4.283
P50895	Basal cell adhesion molecule	15	0.692	0.876	5.378	2.493	2.363	3.936	2.864
P78310	Coxsackievirus and adenovirus receptor	3	1.773	3.140	5.228	16.042	4.507	3.265	3.256
Q10589	Bone marrow stromal antigen 2	2	n.d.	6.438	85.276	94.318	87.278	3.435	38.946
Q14126	Desmoglein-2	9	2.360	3.199	1.912	2.827	5.286	2.542	4.637
Q9H5V8	CUB domain-containing protein 1	2	0.907	2.234	11.680	3.508	11.603	8.623	17.020
Q9Y624	Junctional adhesion molecule A	1	4.374	17.088	25.645	47.784	23.673	77.025	18.523

The iTRAQ ratios were calculated comparing the endometrial cancer cells' iTRAQ signal divided by the normal endometrial cells' iTRAQ signal. Proteins overexpressed more than twofold in at least four cell lines are listed.
Abbreviations: n.d. = Not detected.

HEC-88nu or SNG-II cells (BST2-expressing endometrial cancer cell lines) were assigned to one of three treatment groups ($n = 6$ per group): (i) PBS; (ii) isotype control; (iii) anti-BST2 antibody, 5 mg/kg (SNG-II) or 10 mg/kg (HEC-88nu) twice weekly. Although the tumors of all mice were approximately equal in initial volumes, significant differences in tumor growth were observed during the study, as illustrated by the tumor growth curve in Figure 4a. All mice were sacrificed on days 61 (HEC-88nu) or 85 (SNG-II) post-tumor inoculation. The tumors of the anti-BST2 antibody treatment group were markedly smaller than that of the PBS and control IgG treatment groups (Fig. 4b). The tumor weights of the anti-BST2 antibody treatment group were significantly decreased compared with the PBS and control IgG treatment groups, whereas there was no statistical difference between the PBS and control IgG treatment groups at the termination of the experiment (Fig. 4c).

Once we had established a proof of principle that the anti-BST2 antibody can inhibit tumor growth, we then sought to identify mechanisms by which the anti-BST2 antibody acts on tumor cells. Anti-BST2 antibody treatment showed no significant therapeutic effect in identically treated NOD/SCID mice, with anti-BST2 antibody treated mice developing tumors at virtually the same rate as PBS and control IgG treated mice (Fig. 5).

Discussion

Our study focused on a novel biotechnological method we found to be useful for identifying tumor-associated cell-surface antigens differentially expressed in cancer cells with respect to corresponding normal cells. The ideal expression pattern of a tumor-specific antigen for antibody therapy is that it should be abundant and homogeneous on the surface of cancer cells, and absent from normal tissue.[19] Such targets can be experimentally identified at different molecular levels, such as DNA, RNA, and protein.

DNA microarray technologies have led to the identification of genes that are dysregulated in cancer cells when compared with normal cells.[20,21] However, DNA arrays measure only the changes at the mRNA level, and this is not always translated to corresponding changes at the protein level, leading to many false positives and missed positives. The use of mRNA expression patterns by themselves is often insufficient for understanding the expression of protein products, as additional post-translational mechanisms, including protein translation, post-translational modification, and degradation, may influence the level of a protein and its antigenic epitopes.[22,23] In addition, effective induction of ADCC or CDC mediated by a therapeutic antibody requires abundant expression of cell-surface proteins specifically on the cancer cells,[24,25] providing a compelling rationale for a more direct analysis of gene expression at the protein level by proteomic methods.

The intensity of individual proteins in the sample is crucial when performing proteomic analyses, as larger amounts
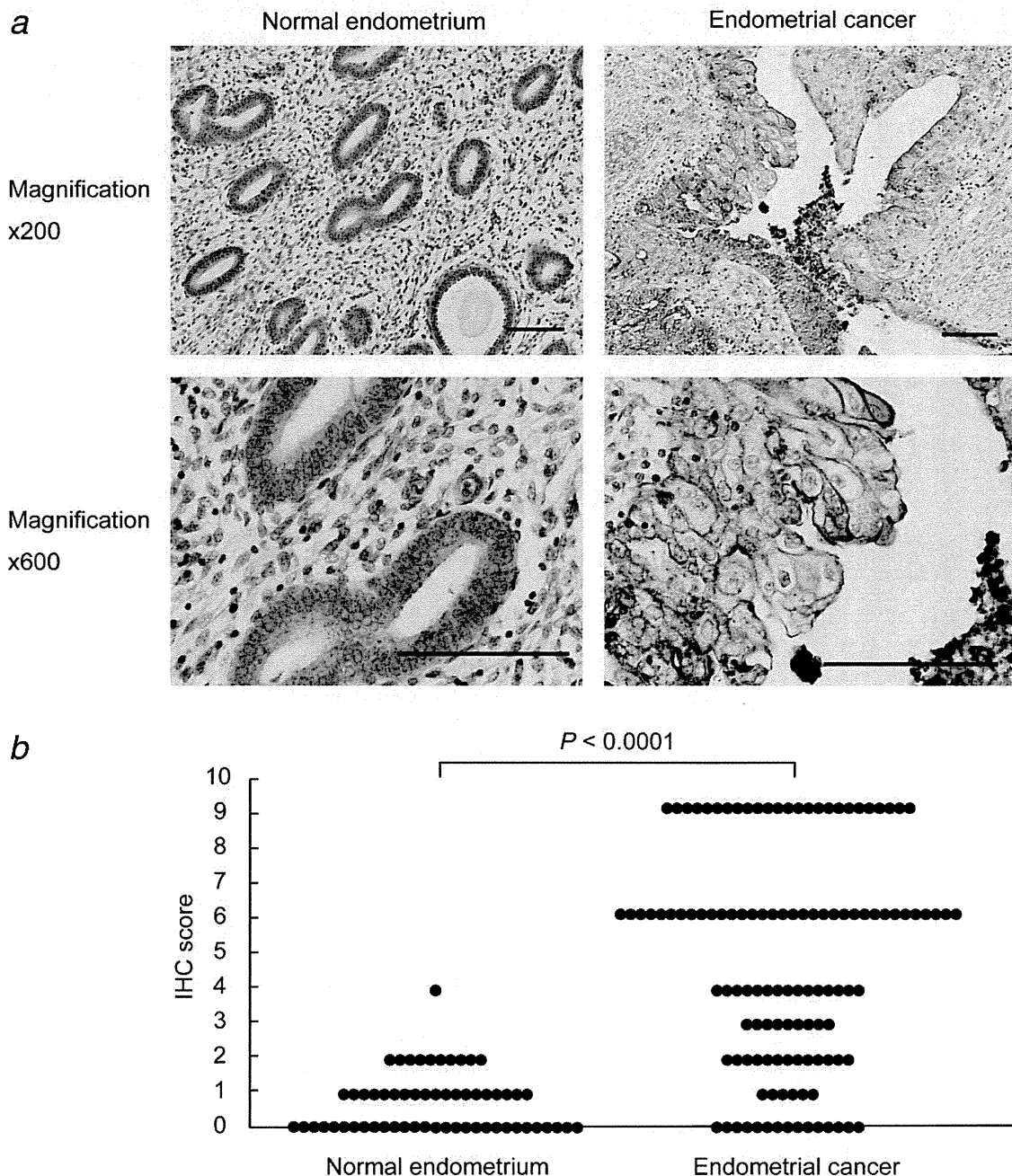
a

b

Figure 2. (*a*) Representative immunohistochemical staining for BST2 in normal endometrium and endometrial cancer specimens. Immunostained sections were counterstained with hematoxylin and photographed with an Olympus FSX100 (Olympus). The expression of BST2 was negative in normal endometrium, whereas endometrial cancer showed strong membranous reactivity for BST2. Scale bar, 100 μm. (*b*) BST2 immunoreactivity in normal endometrial tissues and endometrial cancer tissues. The expression of BST2 was increased in endometrial cancer, with significant difference ($p < 0.0001$). IHC score = intensity score (0, 1, 2, or 3) × positivity score (0, 1, 2, or 3).

of some proteins may hinder the detection of less abundant proteins, such as cell-surface membrane proteins. As such, enrichment of plasma membrane proteins is an important initial step. Physical isolation of membrane proteins using centrifugation and/or chemical extraction are well-described methods.[26,27] However, these techniques fail to isolate only the cell-surface membrane proteins and usually provide

extracts that consist of all the membrane structures, including those inside the cell (e.g., endoplasmic reticulum, Golgi apparatus, and mitochondrial membranes). The proteins that are found inside the cell will most likely not be accessible to the systemically delivered antibodies and hence do not represent a group of interest for discovery of targetable molecules. Another way to enrich specifically the potentially accessible
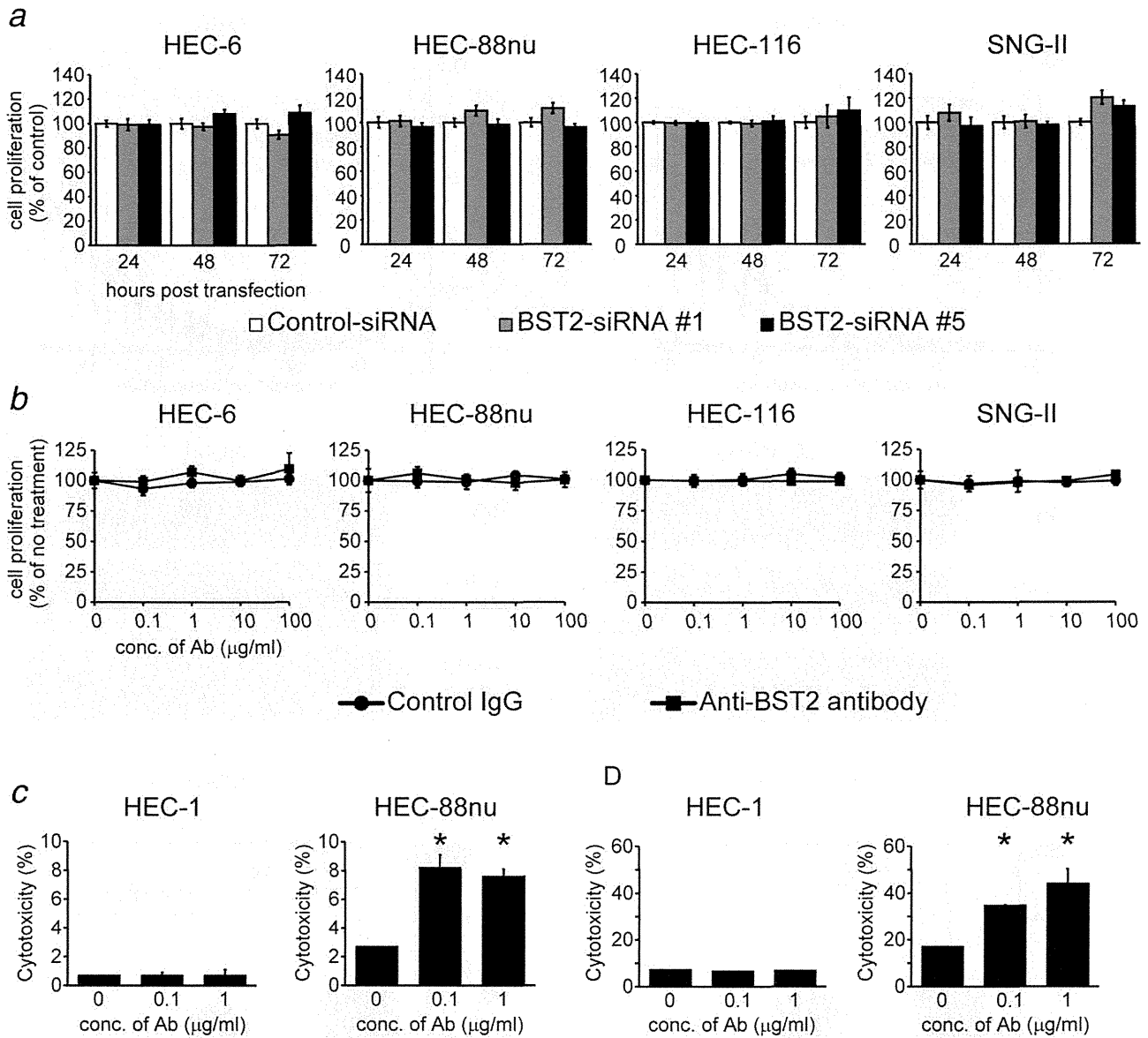
Figure 3. *In vitro* growth assay of endometrial cancer cells treated with BST2-siRNA (*a*) or anti-BST2 antibody (*b*). HEC-6, HEC-88nu, HEC-116, and SNG-II cells are BST2-positive endometrial cancer cell lines. (*a*) A total of 1,000 cells were plated in each well of 96-well plates and then siRNA was transfected. Cell proliferation was assessed at 24, 48, and 72 hr using a WST-8 assay. Values were normalized to control-siRNA treated cells. There were no significant differences in cell proliferation among BST2-siRNA and control-siRNA treated cells. (*b*) Anti-BST2 antibody or isotype-control IgG (final concentrations of 0.1, 1, 10, or 100 μg/ml) were added to 1,000 cells/well in 96-well plates. Cell proliferation was assessed at 72 hr using the WST-8 assay. Values were normalized to untreated cells. Anti-BST2 antibody had no direct cytotoxic effect on endometrial cancer cells *in vitro*. (*c*), ADCC activity of anti-BST2 antibody. Calcein-labeled HEC-1 (BST2-negative) and HEC-88nu (BST2-positive) cells were incubated with bone marrow-derived lymphokine-activated killer cells at an *E/T* ratio of 50 in the presence of 0, 0.1, or 1.0 μg/ml anti-BST2 antibody. (*d*) CDC activity of anti-BST2 antibody. ^{51}Cr-labeled HEC-1 (BST2-negative) and HEC-88nu (BST2-positive) cells were incubated with 12.5% baby rabbit complement in the presence of 0, 0.1, or 1.0 μg/ml anti-BST2 antibody. Anti-BST2 antibody had ADCC and CDC activity against HEC-88nu cells (BST2-expressing endometrial cancer cell line). *$p = 0.045$.

cell-surface proteins involves conjugating membrane proteins with the small molecule biotin and using the receptor streptavidin to extract the labeled proteins.[28,29]

In this study, we quantitatively analyzed the plasma membrane profiles comparing normal endometrium and endometrial cancer using a biotinylation-based approach for cell membrane enrichment combined with iTRAQ technology using nano LC-MS/MS analysis. While quantitative membrane proteomic approaches combining biotin labeling followed by enrichment of cell surface membrane proteins by avidin-beads and SILAC technology or spectral counting were already reported,[28,30] we demonstrated that iTRAQ approach is also an alternative method, suitable for the quantitative analysis of the cell surface membrane proteins.
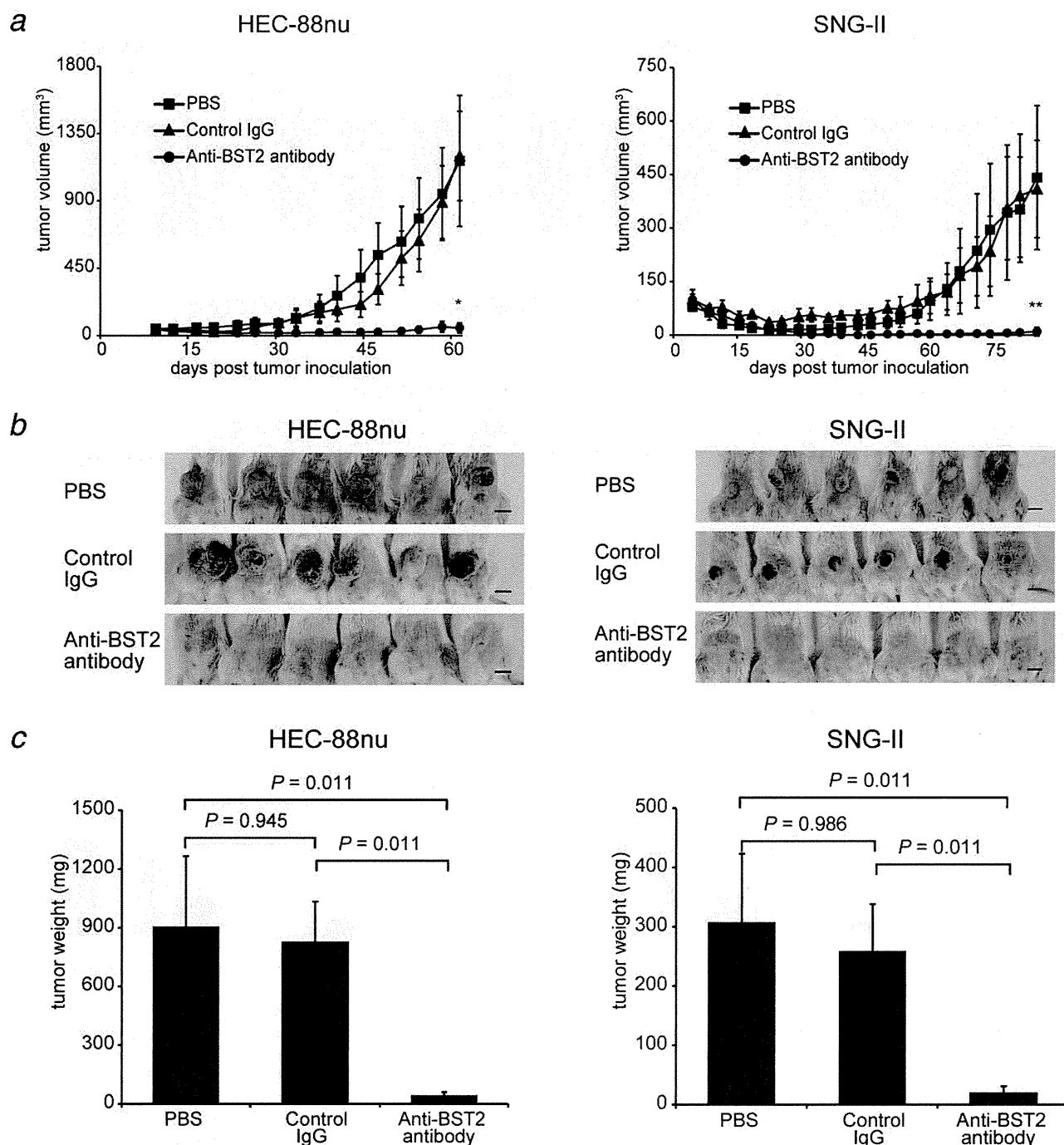
a

b

c

Figure 4. *In vivo* therapeutic effect of anti-BST2 antibody on endometrial cancer growth. SCID mice inoculated with HEC-88nu or SNG-II cells (both are BST2-expressing endometrial cancer cell lines) received PBS, control IgG, or anti-BST2 antibody twice a week for 4 weeks from days 4 (SNG-II) or 9 (HEC-88nu) post-tumor inoculation. (*a*) Time-course of tumor volume change. Tumor volumes were measured twice a week and calculated as the product of length, width, and height. The mean volume ± SD of six tumors in each group is shown. Anti-BST2 antibody treatment resulted in significantly decreased tumor growth compared with the other control groups (PBS and control IgG) at the termination of the experiment. *p = 0.0110, **p = 0.0108. (*b*) Mice at the end of the experiment. Scale bar, 1 cm. (*c*) Tumor weight at autopsy. After 4 (HEC-88nu) or 8 (SNG-II) weeks of observation following treatment, tumors were removed and weighted. Their weights were significantly different between the experimental (anti-BST2 antibody) group and the control (PBS and control IgG) groups (p = 0.011).

In total, we identified 272 proteins, 139 of which (51%) were found to be cell-surface proteins. Given that global genomic analysis predicts that 20 to 30% of all open reading frames encode integral membrane proteins,[31] our results indicate that the membrane proteins were moderately enriched by our sample preparation strategy.
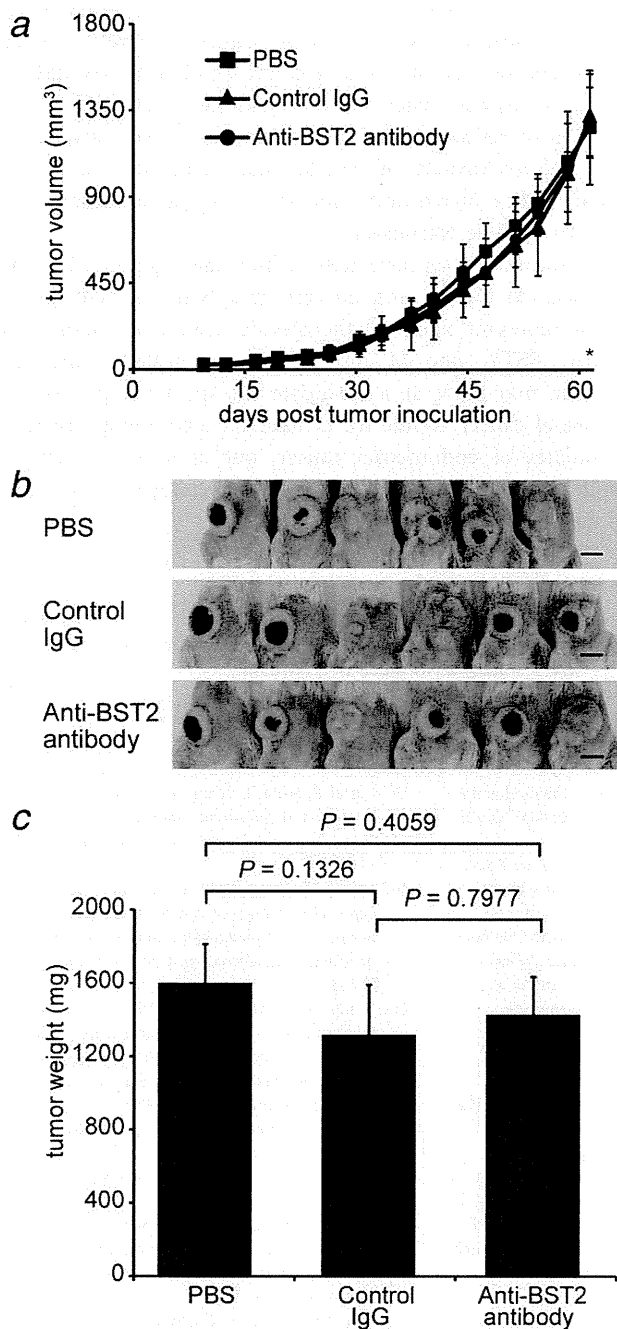
Figure 5. Natural killer cells are required for antitumor activity of anti-BST2 antibody *in vivo*. NOD/SCID mice inoculated with HEC-88nu cells (BST2-expressing endometrial cancer cell line) received PBS, control IgG, or anti-BST2 antibody twice a week for 4 weeks from day 9 post-tumor inoculation. (*a*) Time-course of tumor volume change. Tumor volumes were measured twice a week and calculated as the product of length, width, and height. The mean volume ± SD of six tumors in each group is shown. There were no significant differences in tumor volumes among PBS, control IgG, and anti-BST2 antibody groups at the termination of the experiment. *$p = 0.9769$. (*b*) Mice at the end of the experiment. Scale bar, 1 cm. (*c*) Tumor weight at autopsy. After 4 weeks of observation following treatment, tumors were removed and weighted. There were no significant differences in tumor weights among the three groups.

Eleven proteins were annotated as unique membrane proteins whose expression was specifically up-regulated in endometrial cancer (Table 1). These proteins included several reported markers for prediction of clinical outcome (neural cell adhesion molecule L1 and CUB domain-containing protein 1), suggesting a certain amount of robustness for our methodology of identifying tumor-associated antigens.[32,33] In the present study, BST2 was further validated as a potential therapeutic target for endometrial cancer, because BST2 showed one of the most significant differences between normal endometrium and endometrial cancer (a 10-fold up-regulation was shown in four of seven endometrial cancer cell lines compared with the normal endometrial cell line) and has been reported to be overexpressed in endometrial cancer using genome-wide gene expression profiling.[21] In future work, we would like to characterize other novel candidates for developing new therapeutic agents.

BST2 (also termed CD317, tetherin, or HM1.24) was originally identified as a Type II membrane glycoprotein with an unusual topology (one-pass transmembrane domain and C-terminal glycosylphosphatidylinositol anchor) that is preferentially overexpressed on multiple myeloma cells.[34,35] More recently, BST2 has also been proposed as a tumor-associated antigen expressed in some human cancer cell lines.[36–38] However, BST2 is an interferon-induced protein and inflammatory cytokines such as interleukin-6 and tumor necrosis factor-alpha might also induce its expression.[35] Furthermore, BST2 has been found to block the release of enveloped virus particles (e.g., HIV-1, Marburg virus, and Ebola virus) and may therefore be an important component of the antiviral innate immune defense.[39,40] Future research should further explore the role of BST2 in inflammatory diseases.

To our knowledge, protein expression of BST2 in endometrial cancer has not been described before. Our results are the first to show that BST2 is significantly overexpressed in endometrial cancer compared with normal endometrium. The degree of histological differentiation and surgical pathological staging showed no significant correlation with expression of BST2. Given the almost ubiquitous expression of BST2 in endometrial cancer, BST2 might have some value acting as a potential molecular therapeutic target.[19] In this study, we demonstrated that the administration of the anti-BST2 antibody reduced the growth of BST2-positive endometrial cancer cells in SCID mice. The suppressive effects on tumor growth were observed in two cell lines. In principle, the putative mechanisms of monoclonal antibody-based cancer therapy can be classified into two categories.[41,42] One mechanism is direct action to block the function of target signaling molecules or receptors, or stimulate apoptosis. It has been reported that BST2 gene is one of the important activators of the NF-κB pathway,[43] suggesting that the signaling from BST2 antigen affects the biological responses of BST2-expressing cells. However, silencing of BST2 expression by siRNA transfection did not alter its cell proliferation, and the anti-BST2 antibody had no direct cytotoxic effect on

BST2-positive endometrial cancer cells *in vitro*. The other mechanism of tumor growth suppression is *via* an indirect action mediated by immune systems such as the ADCC and CDC. We showed that the anti-BST2 antibody had ADCC and CDC activity against BST2-expressing endometrial cancer cells. Indeed, the same clone of this monoclonal antibody used in this study has previously been shown to be effective in promoting ADCC and CDC.[37,38] To examine the relative importance of ADCC, xenograft analysis was performed using NOD/SCID mice,[44] which have impaired natural killer cells, thereby compromising their ADCC activity. Anti-BST2 antibody treatment did not result in a significant decrease in tumor growth, suggesting that host effector mechanisms, and ADCC in particular, critically contribute to the antitumor activity of the anti-BST2 antibody *in vivo*.[45]

Beyond tumors, expression of BST2 on normal tissue is a key factor in assessing the suitability of an antigen for antibody targeting in oncology. Expression of BST2 in normal tissues is still less clear. An earlier report indicated that BST2 expression was barely detectable on normal B cells and was not detected on other normal tissues, including bone marrow, liver, heart, kidney, and spleen.[34] A recent article demonstrated the expression of BST2 in various normal tissues by immunohistochemistry.[46] Although limited, a Phase I clinical study reported that a humanized anti-BST2 antibody did not cause any serious toxicity when administered to patients with relapsed or refractory multiple myeloma.[47,48] To consider the potential for toxicity of targeted anti-BST2 therapies, additional studies in relevant animals, including nonhuman primates, would be warranted.

In summary, we have used a high-throughput proteomic approach to identify and quantify membrane proteins which might represent potential therapeutic targets of endometrial cancer. BST2, one of the proteins identified using this method, may serve as a candidate therapeutic target for endometrial cancer. While we focused on identifying targetable candidates of endometrial cancer, our approach is broadly applicable to other malignancies for screening new therapeutic targets.

Acknowledgements

References

1. Marcus R, Imrie K, Belch A, et al. CVP chemotherapy plus rituximab compared with CVP as first-line treatment for advanced follicular lymphoma. *Blood* 2005;105:1417–23.
2. Slamon DJ, Leyland-Jones B, Shak S, et al. Use of chemotherapy plus a monoclonal antibody against HER2 for metastatic breast cancer that overexpresses HER2. *N Engl J Med* 2001;344: 783–92.
3. Leth-Larsen R, Lund RR, Ditzel HJ. Plasma membrane proteomics and its application in clinical cancer biomarker discovery. *Mol Cell Proteomics* 2010;9:1369–82.
4. Shin BK, Wang H, Yim AM, et al. Global profiling of the cell surface proteome of cancer cells uncovers an abundance of proteins with chaperone function. *J Biol Chem* 2003;278: 7607–16.
5. Zhao Y, Zhang W, Kho Y. Proteomic analysis of integral plasma membrane proteins. *Anal Chem* 2004;76:1817–23.
6. Ong SE, Blagoev B, Kratchmarova I, et al. Stable isotope labeling by amino acids in cell culture, SILAC, as a simple and accurate approach to expression proteomics. *Mol Cell Proteomics* 2002; 1:376–86.
7. Alex P, Gucek M, Li X. Applications of proteomics in the study of inflammatory bowel diseases: current status and future directions with available technologies. *Inflamm Bowel Dis* 2009; 15:616–29.
8. Choe L, D'Ascenzo M, Relkin NR, et al. 8-plex quantitation of changes in cerebrospinal fluid protein expression in subjects undergoing intravenous immunoglobulin treatment for Alzheimer's disease. *Proteomics* 2007;7: 3651–60.
9. Jemal A, Siegel R, Xu J, et al. Cancer statistics, 2010. *CA Cancer J Clin* 2010;60:277–300.

10. Obel JC, Friberg G, Fleming GF. Chemotherapy in endometrial cancer. *Clin Adv Hematol Oncol* 2006;4:459–68.
11. Fleming GF, Brunetto VL, Cella D, et al. Phase III trial of doxorubicin plus cisplatin with or without paclitaxel plus filgrastim in advanced endometrial carcinoma: a Gynecologic Oncology Group Study. *J Clin Oncol* 2004;22:2159–66.
12. Humber CE, Tierney JF, Symonds RP, et al. Chemotherapy for advanced, recurrent or metastatic endometrial cancer: a systematic review of Cochrane collaboration. *Ann Oncol* 2007;18:409–20.
13. Kyo S, Nakamura M, Kiyono T, et al. Successful immortalization of endometrial glandular cells with normal structural and functional characteristics. *Am J Pathol* 2003;163:2259–69.
14. Mizumoto Y, Kyo S, Ohno S, et al. Creation of tumorigenic human endometrial epithelial cells with intact chromosomes by introducing defined genetic elements. *Oncogene* 2006;25:5673–82.
15. Scheurer SB, Rybak JN, Roesli C, et al. Identification and relative quantification of membrane proteins by surface biotinylation and two-dimensional peptide mapping. *Proteomics* 2005;5:2718–28.
16. Roden MM, Lee KH, Panelli MC, et al. A novel cytolysis assay using fluorescent labeling and quantitative fluorescent scanning technology. *J Immunol Methods* 1999;226:29–41.
17. Neri S, Mariani E, Meneghetti A, et al. Calcein-acetyoxymethyl cytotoxicity assay: standardization of a method allowing additional analyses on recovered effector cells and supernatants. *Clin Diagn Lab Immunol* 2001;8:1131–5.
18. Wang W, Nishioka Y, Ozaki S, et al. Chimeric and humanized anti-HM1.24 antibodies mediate antibody-dependent cellular cytotoxicity against lung cancer cells. *Lung Cancer* 2009;63:23–31.

19. Carter P, Smith L, Ryan M. Identification and validation of cell surface antigens for antibody targeting in oncology. *Endocr Relat Cancer* 2004; 11:659–87.
20. Mutter GL, Baak JP, Fitzgerald JT, et al. Global expression changes of constitutive and hormonally regulated genes during endometrial neoplastic transformation. *Gynecol Oncol* 2001;83: 177–85.
21. Wong YF, Cheung TH, Lo KW, et al. Identification of molecular markers and signaling pathway in endometrial cancer in Hong Kong Chinese women by genome-wide gene expression profiling. *Oncogene* 2007;26:1971–82.
22. Chen G, Gharib TG, Huang CC, et al. Discordant protein and mRNA expression in lung adenocarcinomas. *Mol Cell Proteomics* 2002;1: 304–13.
23. Tian Q, Stepaniants SB, Mao M, et al. Integrated genomic and proteomic analyses of gene expression in mammalian cells. *Mol Cell Proteomics* 2004;3:960–9.
24. Mimura K, Kono K, Hanawa M, et al. Trastuzumab-mediated antibody-dependent cellular cytotoxicity against esophageal squamous cell carcinoma. *Clin Cancer Res* 2005;11: 4898–904.
25. van Meerten T, van Rijn RS, Hol S, et al. Complement-induced cell death by rituximab depends on CD20 expression level and acts complementary to antibody-dependent cellular cytotoxicity. *Clin Cancer Res* 2006;12:4027–35.
26. Patwardhan AJ, Strittmatter EF, Camp DG II, et al. Comparison of normal and breast cancer cell lines using proteome, genome, and interactome data. *J Proteome Res* 2005;4:1952–60.
27. Tan S, Tan HT, Chung MC. Membrane proteins and membrane proteomics. *Proteomics* 2008;8: 3924–32.

28. Conn EM, Madsen MA, Cravatt BF, et al. Cell surface proteomics identifies molecules functionally linked to tumor cell intravasation. *J Biol Chem* 2008;283:26518–27.

29. Kischel P, Guillonneau F, Dumont B, et al. Cell membrane proteomic analysis identifies proteins differentially expressed in osteotropic human breast cancer cells. *Neoplasia* 2008;10: 1014–20.

30. Qiu H, Wang Y. Quantitative analysis of surface plasma membrane proteins of primary and metastatic melanoma cells. *J Proteome Res* 2008;7: 1904–15.

31. Wallin E, von Heijne G. Genome-wide analysis of integral membrane proteins from eubacterial, archaean, and eukaryotic organisms. *Protein Sci* 1998;7:1029–38.

32. Fogel M, Gutwein P, Mechtersheimer S, et al. L1 expression as a predictor of progression and survival in patients with uterine and ovarian carcinomas. *Lancet* 2003;362:869–75.

33. Mamat S, Ikeda J, Enomoto T, et al. Prognostic significance of CUB domain containing protein expression in endometrioid adenocarcinoma. *Oncol Rep* 2010;23:1221–7.

34. Goto T, Kennel SJ, Abe M, et al. A novel membrane antigen selectively expressed on terminally differentiated human B cells. *Blood* 1994;84:1922–30.

35. Ohtomo T, Sugamata Y, Ozaki Y, et al. Molecular cloning and characterization of a surface antigen preferentially overexpressed on multiple myeloma cells. *Biochem Biophys Res Commun* 1999;258:583–91.

36. Walter-Yohrling J, Cao X, Callahan M, et al. Identification of genes expressed in malignant cells that promote invasion. *Cancer Res* 2003;63: 8939–47.

37. Kawai S, Azuma Y, Fujii E, et al. Interferon-alpha enhances CD317 expression and the antitumor activity of anti-CD317 monoclonal antibody in renal cell carcinoma xenograft models. *Cancer Sci* 2008;99:2461–6.

38. Wang W, Nishioka Y, Ozaki S, et al. HM1.24 (CD317) is a novel target against lung cancer for immunotherapy using anti-HM1.24 antibody. *Cancer Immunol Immunother* 2009;58: 967–76.

39. Neil SJ, Zang T, Bieniasz PD. Tetherin inhibits retrovirus release and is antagonized by HIV-1 Vpu. *Nature* 2008;451:425–30.

40. Jouvenet N, Neil SJ, Zhadina M, et al. Broad-spectrum inhibition of retroviral and filoviral particle release by tetherin. *J Virol* 2009;83: 1837–44.

41. Adams GP, Weiner LM. Monoclonal antibody therapy of cancer. *Nat Biotechnol* 2005;23: 1147–57.

42. Imai K, Takaoka A. Comparing antibody and small-molecule therapies for cancer. *Nat Rev Cancer* 2006;6:714–27.

43. Matsuda A, Suzuki Y, Honda G, et al. Large-scale identification and characterization of human genes that activate NF-kappaB and MAPK signaling pathways. *Oncogene* 2003;22:3307–18.

44. Shultz LD, Schweitzer PA, Christianson SW, et al. Multiple defects in innate and adaptive immunologic function in NOD/LtSz-scid mice. *J Immunol* 1995;154:180–91.

45. Mulgrew K, Kinneer K, Yao XT, et al. Direct targeting of alphavbeta3 integrin on tumor cells with a monoclonal antibody, Abegrin. *Mol Cancer Ther* 2006;5:3122–9.

46. Erikson E, Adam T, Schmidt S, et al. In vivo expression profile of the antiviral restriction factor and tumor-targeting antigen CD317/BST-2/HM1.24/tetherin in humans. *Proc Natl Acad Sci USA* 2011;108:13688–93.

47. Powles R, Sirohi B, Morgan G, et al. A phase I study of the safety, tolerance, pharmokinetics, antigenicity and efficacy of a single intravenous dose of AHM followed by multiple doses of intravenous AHM in patients with multiple myeloma. *Blood* 2001;98:165A.

48. Tai Y-T, Anderson KC. Antibody-based therapies in multiple myeloma. *Bone Marrow Res* 2011; 2011:924058.

Periostin Facilitates Skin Sclerosis via PI3K/Akt Dependent Mechanism in a Mouse Model of Scleroderma

Lingli Yang[1,2], Satoshi Serada[2], Minoru Fujimoto[2], Mika Terao[1], Yorihisa Kotobuki[1,2], Shun Kitaba[1], Saki Matsui[1], Akira Kudo[3], Tetsuji Naka[2], Hiroyuki Murota[1]*, Ichiro Katayama[1]

1 Department of Dermatology, Osaka University Graduate School of Medicine, Osaka, Japan, 2 Laboratory for Immune Signal, National Institute of Biomedical Innovation, Osaka, Japan, 3 Department of Biological Information, Tokyo Institute of Technology, Yokohama, Japan

Abstract

Objective: Periostin, a novel matricellular protein, is recently reported to play a crucial role in tissue remodeling and is highly expressed under fibrotic conditions. This study was undertaken to assess the role of periostin in scleroderma.

Methods: Using skin from patients and healthy donors, the expression of periostin was assessed by immunohistochemistry and immunoblotting analyses. Furthermore, we investigated periostin$^{-/-}$ (PN$^{-/-}$) and wild-type (WT) mice to elucidate the role of periostin in scleroderma. To induce murine cutaneous sclerosis, mice were subcutaneously injected with bleomycin, while untreated control groups were injected with phosphate-buffered saline. Bleomycin-induced fibrotic changes were compared in PN$^{-/-}$ and WT mice by histological analysis as well as by measurements of profibrotic cytokine and extracellular matrix protein expression levels *in vivo* and *in vitro*. To determine the downstream pathway involved in periostin signaling, receptor neutralizing antibody and signal transduction inhibitors were used *in vitro*.

Results: Elevated expression of periostin was observed in the lesional skin of patients with scleroderma compared with healthy donors. Although WT mice showed marked cutaneous sclerosis with increased expression of periostin and increased numbers of myofibroblasts after bleomycin treatment, PN$^{-/-}$ mice showed resistance to these changes. *In vitro*, dermal fibroblasts from PN$^{-/-}$ mice showed reduced transcript expression of alpha smooth actin and procollagen type-I alpha 1 (Col1α1) induced by transforming growth factor beta 1 (TGFβ1). Furthermore, recombinant mouse periostin directly induced Col1α1 expression *in vitro*, and this effect was inhibited by blocking the αv integrin-mediated PI3K/Akt signaling either with anti-αv functional blocking antibody or with the PI3K/Akt kinase inhibitor LY294002.

Conclusion: Periostin plays an essential role in the pathogenesis of Bleomycin-induced scleroderma in mice. Periostin may represent a potential therapeutic target for human scleroderma.

Introduction

Scleroderma is a connective tissue disorder with unknown etiology. The disease is characterized by excessive deposition of collagen and other extracellular matrix (ECM) proteins, resulting in fibrosis of skin and other visceral organs [1]. To date, despite much effort, there is still no established treatment for fibrosis in scleroderma.

The ECM of the skin is composed not only of structural proteins such as collagen type-I but of many different proteins that modulate cellular behavior. The interactions among various ECM proteins provide molecular signals to resident cells including dermal fibroblasts and play essential roles in the maintenance and turnover of the ECM. At present, ECM proteins are considered as key players in the pathogenesis of scleroderma.

Among ECM proteins, the cytokine transforming growth factor β1 (TGFβ1) is regarded as a master regulator of the disease

process in scleroderma, since it potently accelerates fibrosis in skin by inducing collagen production; various pro-fibrotic ECM proteins such as CCN2 (also known as a connective tissue growth factor or CTGF) are known to induce the transdifferentiation of fibroblasts to myofibroblasts [2,3]. Recently, a class of ECM proteins called matricellular proteins has attracted increasing attention in the field of scleroderma research. These proteins specifically regulate cell-matrix interactions and play critical roles in embryonic development as well as in tissue repair and fibrosis. Indeed, several matricellular proteins, including CCN2 [4], CCN1 (cysteine-rich protein 61) [5], and their cell-adhesive receptor, integrin β1 [6], have been shown to play roles in scleroderma, and such studies are still ongoing. Thus, investigations of the functions of ECM proteins and their signaling networks are urgently needed to elucidate the pathogenesis of scleroderma and develop new therapies.
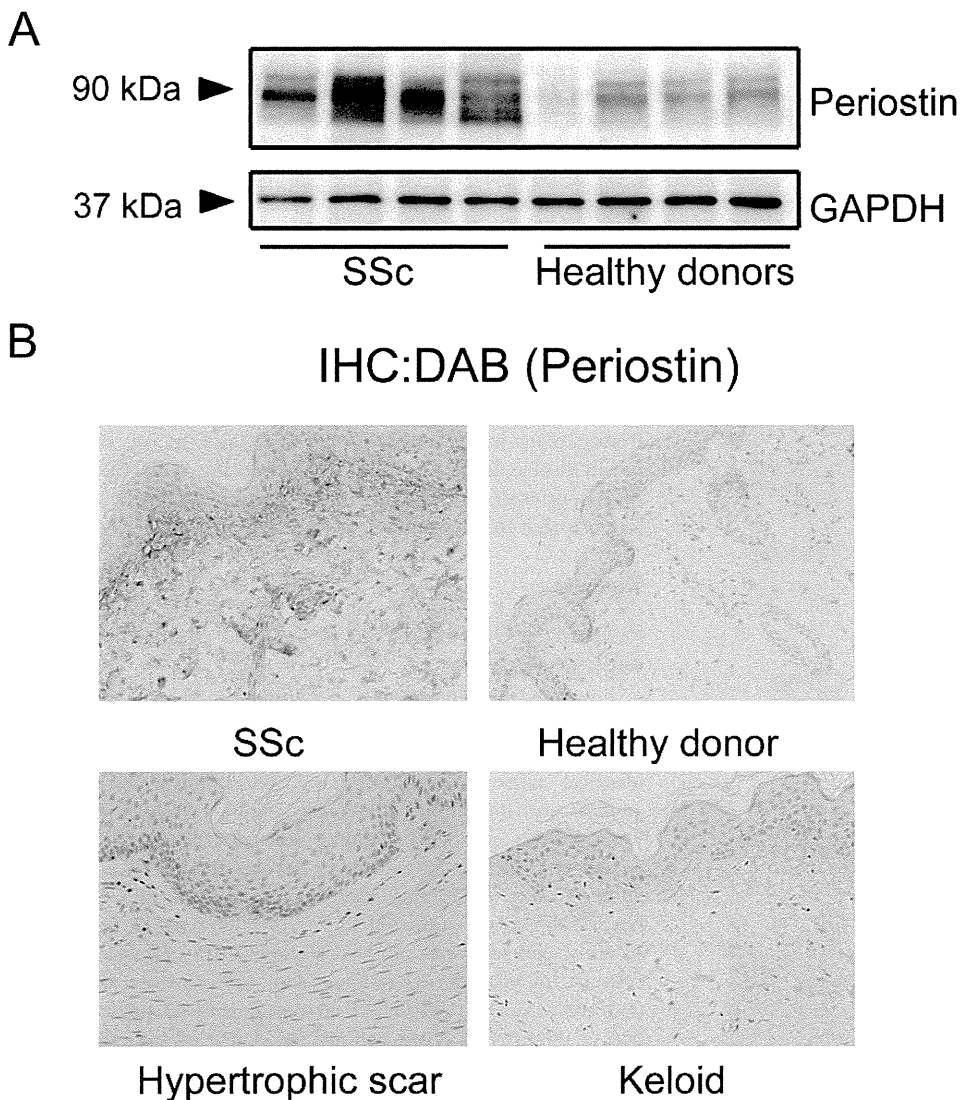
410

A

90 kDa ▶ [Western blot: Periostin]

Periostin

37 kDa ▶ [Western blot: GAPDH]

GAPDH

SSc   Healthy donors

B

IHC:DAB (Periostin)

SSc   Healthy donor

Hypertrophic scar   Keloid

Figure 1. Periostin is overexpressed in lesional skin derived from patients with systemic scleroderma (SSc). A, Western blotting analysis for periostin using protein extracts from the skin of SSc patients and healthy donors. B, Representative immunohistochemistry of skin sections of SSc patients, healthy donors, hypertrophic scar and keloid patients. Slides were stained with anti-periostin antibodies (original magnification, ×100).
doi:10.1371/journal.pone.0041994.g001

To investigate the involvement of matricellular proteins in the pathogenesis of scleroderma, we focused on a novel matricellular protein, periostin, a 90-kDa, secreted, homophilic cell adhesion protein. Despite being first identified 15 years ago as osteoblast-specific factor-2 [7], periostin is now classified as a matricellular protein, because it is expressed in many collagen-rich tissues and possesses important biological functions in the ECM [8]. Periostin can bind to collagen during fibrillogenesis, thus affecting the diameter of collagen fibers and the extent of cross-linking [9,10]. Periostin also binds to other ECM proteins, including fibronectin and tenascin-C, thereby organizing the ECM architecture. Like other matricellular proteins, such as CCN1, CCN2, and CCN3 (capable of interacting with αv, β3, and β1 integrins) [11], periostin serves as a ligand for integrins αv, β1, β3, β4, and β5 [12–14]. Such signals can mediate cell adhesion to the ECM and may regulate certain cellular behaviors, including intracellular signaling, proliferation, and differentiation [15].

Analysis on periostin$^{-/-}$ (PN$^{-/-}$) mice revealed that this protein plays a pivotal role in the development of heart, bones, and teeth [16]. Approximately 14% of PN$^{-/-}$ mice die postnatally prior to weaning [17], suggesting a role of periostin in the development of these tissues. In adults, periostin is prominently upregulated during ECM remodeling and fibrosis. The major producers of periostin are fibroblasts [18,19], and its expression is induced by various factors, including TGFβ1, interleukin (IL) 4, and IL13 [19,20]. The prominent expression of periostin has been detected during a number of remodeling processes, including myocardial infarction [21], wound repair [8,22–24], fibrotic scar formation [25], sub-epithelial fibrosis in bronchial asthma [20], and bone marrow fibrosis [26]. Studies of PN$^{-/-}$ mice with experimentally induced diseases have further confirmed that periostin, in many cases, is profoundly involved in the progression of tissue fibrosis [17,27–29]. However, in a model of bronchial asthma, PN$^{-/-}$ mice developed peribronchial fibrosis equivalent

411

PN$^{-/-}$ mice (original magnification, ×100). Dermal thickness is shown as the black bar in the lower panel and was measured as described in the Materials and Methods. C, Masson's trichrome staining of skin samples from WT and PN$^{-/-}$ mice (original magnification, ×100). Collagen fibers were stained blue. Collagen deposition was scored on a scale of 0–3 as described in the Materials and Methods and is shown in the lower panel. For all assays, 10 mice from each group were analyzed. Values in B and C are shown as the mean ± SD. NS, no significance; ***, p<0.01.
doi:10.1371/journal.pone.0041994.g002

to WT mice [30], suggesting that periostin plays a limited role or is dispensable in certain conditions of fibrosis.

At present, it is unclear whether periostin is upregulated in the fibrotic lesions of scleroderma or plays a role in its pathology. In the present study, we analyzed periostin expression in skin samples from patients with systemic scleroderma, and the role of periostin in this disease, using PN$^{-/-}$ mice in a murine model of bleomycin (BLM)-induced scleroderma that exhibits defined cutaneous sclerosis that mimics human scleroderma [31].

Results

Periostin is Overexpressed in Lesional Skin of Patients with Scleroderma

To assess the involvement of periostin in the pathogenesis of scleroderma, we first compared the expression of periostin in sclerotic skin lesions from scleroderma patients and skin from identical areas of healthy donors. Based on western blotting analysis and immunohistochemical staining, periostin expression was markedly elevated in lesional skin from scleroderma patients compared with skin from healthy donors (Figure 1A and 1B). In addition, the distribution pattern of periostin in normal and fibrotic skin tissue appeared to be very different. In normal skin sections, periostin was faintly detectable in the upper dermis. In contrast, in scleroderma lesional skin, more intense staining for periostin was observed in the surrounding ECM throughout the dermis (Figure 1B). Furthermore, we examined periostin expression in the lesional skin from patients with other skin fibrotic diseases (keloid and hypertrophic scar), and found that periostin appeared to be expressed more strongly in lesional skin tissue of scleroderma than in those of keloid and hypertrophic scar (Figure 1B).

Periostin Gene Knockout Results in Reduced Symptoms of BLM-induced Cutaneous Sclerosis in Mice

Given these results above, it was logical to ask whether periostin plays an essential role in the pathophysiology of scleroderma or whether the altered expression of periostin is secondary to the disease process. To resolve this issue, we assessed the role of periostin in BLM-induced murine scleroderma using PN$^{-/-}$ mice [27]. To induce cutaneous sclerosis, we subcutaneously injected mice with BLM or PBS for four consecutive weeks, which has been widely used as an animal model of scleroderma [31]. Skin samples were collected one day after the final injection. To evaluate whether periostin is overexpressed in mice with BLM-induced scleroderma, the proteins extracted from mouse skin were subjected to western blotting analysis (Figure 2A). Indeed, periostin was strongly expressed in BLM-induced sclerotic skin of WT mice compared to skin samples from control PBS-treated mice. Antibody specificity was confirmed by the absence of a corresponding band in samples from PN$^{-/-}$ mice. These results agree with the supposition that elevated expression of periostin is closely linked to the pathogenesis of scleroderma.
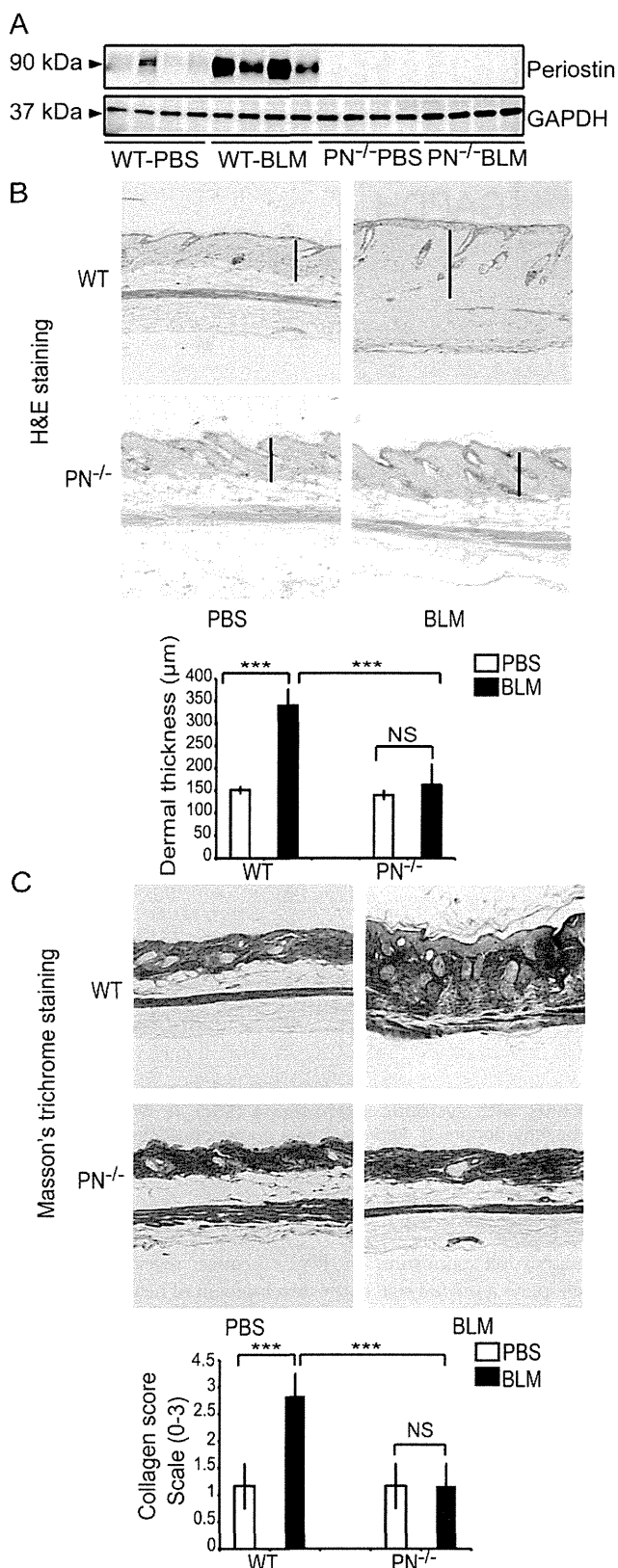
Figure 2. Periostin gene knockout (PN$^{-/-}$) mice are resistant to BLM-induced cutaneous sclerosis as assessed by dermal thickness and collagen deposition. A, Western blotting analysis for periostin in skin extracts from WT and PN$^{-/-}$ mice, which were treated with BLM or PBS. B, H&E staining of skin samples from WT and

412

Next, histological examinations of mouse skin sections using H&E staining (Figure 2B) were performed. As previously reported in this mouse model [32], a striking increase in dermal thickness and an apparent decrease in the amount of subcutaneous fat tissue (Figure 2B) were observed in WT mice injected with BLM. In contrast, PN$^{-/-}$ mice showed minimal dermal thickening (Figure 2B). WT mice showed a statistically significant increase of 220% ±33% in dermal thickness following BLM treatment (p<0.01), whereas, PN$^{-/-}$ mice did not develop apparent dermal thickening (Figure 2B, bar graph, lower panel).

Masson's trichrome staining, which stains collagen fibers blue, was performed to examine the increase of collagen fibers in BLM-treated mice (Figure 2C). WT BLM-treated mice displayed substantial thickening of the dermis with a robust deposition of collagen fibers that replaced the subcutaneous fat. These changes were markedly attenuated in BLM-treated PN$^{-/-}$ mice. Assessment using a four-point (grade 0–3) collagen deposition scoring system confirmed that the difference between PN$^{-/-}$ mice and WT mice was significant (Figure 2C, bar graph, lower panel).

Collectively, these results demonstrate that PN$^{-/-}$ mice display markedly reduced symptoms of BLM-induced cutaneous sclerosis, indicating that periostin is required for the development of BLM-induced cutaneous sclerosis.

Expression of Fibrogenic Cytokines and ECM Proteins in BLM-treated Mice Skin

Next, we assessed the expression of the main fibrogenic cytokines, TGFβ1 and CCN2 (also called CTGF), by real-time quantitative PCR. The expression of TGFβ1 and CCN2 (CTGF) mRNA after BLM treatment (Figure 3A and 3B) was increased in both WT and PN$^{-/-}$ mice, suggesting that the fibrotic process was initiated similarly in both PN$^{-/-}$ and WT mice. We then assessed the mRNA levels of Col1α1, a major component of dermal collagen fibers in these mice. Col1α1 mRNA levels were increased (536±76%) in WT mice skin after BLM treatment (p<0.01), but unexpectedly, not in BLM-treated PN$^{-/-}$ mice (Figure 3C). Thus, while periostin is known to regulate collagen assembly [10], these data suggest that periostin in BLM-induced scleroderma is critical for excessive collagen synthesis.

Periostin is Required for Myofibroblast Differentiation *in vivo*

It is widely accepted that α-SMA-expressing myofibroblasts, which are induced by fibrogenic cytokines, play key roles in collagen synthesis during the development of scleroderma [33]. To determine whether periostin is required for myofibroblast differentiation in this model, histoimmunohistochemistry for α-SMA (the most widely used myofibroblast marker) was performed on skin derived from WT and PN$^{-/-}$ mice with BLM or after PBS treatment (Figure 4A). α-SMA$^+$ cells were increased in the dermis of skin sections from BLM-treated WT mice compared with skin from PBS-treated WT mice (Figure 4A). In contrast, α-SMA$^+$ cells were not increased in BLM-treated PN$^{-/-}$ mice (Figure 4A). To detect myofibroblasts more specifically, double-labeling histoimmunofluorescence staining for anti-α-SMA and anti-CD34 (a representative vascular endothelial maker) were further performed (Figure 4B). Nonvascular α-SMA-positive CD34-negative spindle-shaped cells (α-SMA$^+$ and CD34$^-$ cells), which indicate myofibroblasts, increased in the dermis of WT mice with statistical significance (p<0.01) but not in PN$^{-/-}$ mice (Figure 4C) after BLM treatment.

Supporting these data, western blotting analysis revealed an increase in the expression of α-SMA in skin derived from BLM-treated WT mice, but not PN$^{-/-}$ mice, compared with PBS-treated WT mice (Figure 4D). These results suggest that periostin is required for myofibroblast development in this scleroderma model.

Periostin is Required for TGFβ1-induced Myofibroblast Differentiation *in vitro*

TGFβ1 is the most potent inducer of myofibroblast differentiation in fibrosis [34]. To investigate the mechanism of action of periostin in myofibroblast generation, we isolated mouse dermal fibroblasts from WT and PN$^{-/-}$ mice and stimulated these cells with TGFβ1 *in vitro*. The induction of α-SMA at 2 hrs after TGFβ1 stimulation appeared similar between WT and PN$^{-/-}$ fibroblasts. However, after longer periods of stimulation (12 hrs, 24 hrs), α-SMA expression levels in PN$^{-/}$
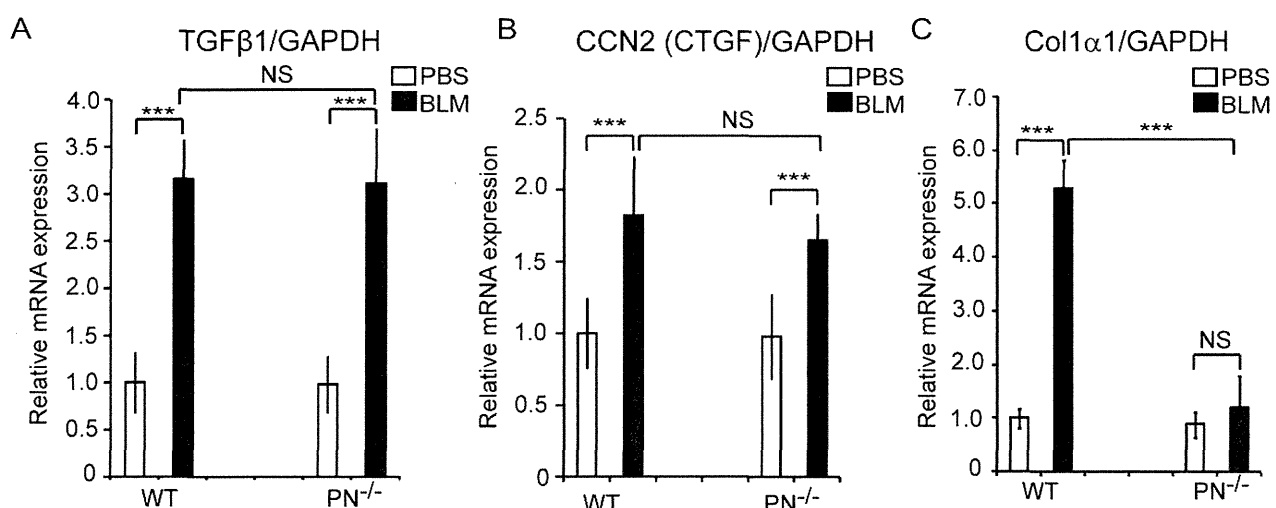

Figure 3. The expression of fibrogenic cytokines (TGFβ1 and CCN2/CTGF) and collagen type I in BLM-treated mouse skin. Real-time quantitative PCR analysis was performed to determine mRNA levels of TGFβ1 (A), CCN2 (CTGF) (B), and Col1α1 (C) in mouse skin of WT and PN$^{-/-}$ mice. Values were normalized to GAPDH levels and expressed as relative mRNA levels compared with PBS-treated WT mice. Values are shown as the mean ± SD. NS, no significance; ***, p<0.01.
doi:10.1371/journal.pone.0041994.g003